Controlled Release from and Tissue Response to Physically Bonded Hydrogel Nanoparticle Assembly

Zhibing Hu,[1] Xiaohu Xia,[1] Manuel Marquez,[2+] Hong Weng,[3] Liping Tang[3]*

[1] Departments of Physics and Chemistry, University of North Texas, P. O. Box 311427, Denton, Texas 76203, USA
E-mail: zbhu@unt.edu
[2] Los Alamos National Laboratory, Chemistry Division, Los Alamos, New Mexico 87545, USA
[3] Biomedical Engineering Program, University of Texas at Arlington, P.O. Box 19138, Arlington, Texas 76019, USA

Summary: Our recent work on synthesis and application of thermally gelling nanoparticle dispersions is briefly reviewed here. These nanoparticles consist of interpenetrating polymer networks (IPN) of poly-acrylic acid (PAAc) and poly(*N*-isopropylacrylamide) (PNIPAM). The aqueous IPN nanoparticle dispersions with polymer concentrations above 2.5 wt % underwent an inverse thermoreversible gelation at about 33 ^{0}C. Dextran markers of various molecular weights as model macromolecular pseudodrugs were mixed with the IPN nanoparticle dispersion at room temperature. At body temperature, the dispersion became a gel. The dextran release profiles were then measured using UV-visible spectroscopy. The biocompatibility of this nanoparticle assembly was assessed using an animal implantation model.

Keywords: biocompatibility; drug delivery systems; gelation; hydrogels; nanoparticles

Introduction

Polymeric systems that form gels have been studied via sol-gel transitions without chemical reaction.[1] Thermoreversible gelation has been reported for gelatin and polysaccharides.[2-3] More interesting, but more rare, are systems that have an inverse thermoreversible gelation (i.e. gelation at elevated temperatures).[4] These polymer solutions include chitosan,[5] poly(ethylene oxide)-poly(propylene oxide)-poly(ethylene oxide) triblock copolymers (Pluronic or Poloxamer),[6] poly-isopropylacrylamide (PNIPAM) and polyacrylic acid (PAAc) copolymers,[7] and degradable triblock copolymers.[4] In contrast to these polymer solutions, a novel aqueous dispersion of

[+] I'NEST group - New Technology Research Department, PMUSA, Richmond, VA, 23298, USA.

 DOI: 10.1002/masy.200550927

hydrogel nanoparticles has been synthesized recently.[8-10] This dispersion is a fluid at room temperature but becomes a gel above about 33 ^{0}C. The hydrogel nanoparticles consist of polymer interpenetrating networks of PNIPAM and PAAc. The PNIPAM provides physical crosslinking bonds between particles via a temperature-dependent interparticle potential, while PAAc in the neutral pH provides repulsive ionic charges that are temperature-independent and prevent the collapse of the particles into an aggregate.

Hydrogel nanoparticles have been previously used as building blocks to form a 3D network by crosslinking neighboring particles.[11-12] However, introduction of crosslinker agents may affect the stability of entrapped biomedical drug in some cases. The formation of a hydrogel nanoparticle network described here relies on physically interparticle attractive force created largely by hydrophobic and van der Waals interaction.[8-10] In our system, no crosslinker or chemical reaction is needed to bond neighboring particles. A pseudodrug molecule can be mixed into the nanoparticle dispersion at room temperature. At body temperature (37 ^{0}C), the particles are linked by hydrophobic interaction to form a gel, that allows the pseudodrug to diffuse out slowly. Because there is no chemical reaction involved, a protein or other reactive drug molecule can be entrapped in the nanoparticle network safely. Since it is essential for a biomaterial implant to possess good biocompatibility, the tissue compatibility of these nanoparticles was tested by injecting the particle dispersion into the subcutaneous cavity of mice. After implantation for seven days, the implants and surrounding tissues were recovered for histological analyses.

Experimental

PNIPAM nanoparticle preparation: PNIPAM nanoparticles were synthesized following the methods of Pelton and Chibante.[13] 3.8 g N-isopropylacrylamide, 0.066 g N, N'-Methylenebisacrylamide and 0.15 g sodium dodecyl sulfate (SDS) were dissolved in 240 g distilled water under a nitrogen environment. 0.166 g potassium persulfate, which was dissolved in 20 ml water, was then added to initiate polymerization. The reaction temperature was kept at 70±1 °C. The PNIPAM nanoparticles with hydrodynamic radii of 125 nm were obtained and were hereafter named as PNIPAM125.

IPN nanoparticle synthesis: The IPN nanoparticles were prepared using above PNIPAM nanoparticles as seeds.[8-10] 35 g PNIPAM nanoparticle dispersion that was diluted ten times with distilled water was mixed with 0.5 g N, N'-methylenebisacrylamide and 2.3 g acrylic acid under nitrogen environment. The initiator (0.2 g ammonium persulfate) and

accelerator (0.2 g TEMED) were separately dissolved in water and added rapidly to the solution, making the final solution volume to 370 ml. The reaction was carried out under nitrogen atmosphere at 23°C. The polymerization reaction lasted for 23 mins and the resultant IPN nanoparticles were purified by dialysis and ultracentrifugation. Their average hydrodynamic radius at 23°C was 155 nm as measured by dynamic light scattering (DLS), and hereafter named as IPN155.

Implantation of materials: As an in vivo model for evaluating biomaterial-mediated tissue reactions, the IPN nanoparticle assembly was implanted subcutaneously in Balb/C mice (about 20 gram body weight) from Taconic Farms, Inc. (Germantown, NY). Briefly, test materials (3 mg dry weight/300 μl/mouse) were administrated into subcutaneous space (on the back) of mice. After implantation for seven days, the implants and surrounding tissues were recovered, frozen sectioned, and then histologically analysed.

Histochemical analyses: After sectioning with Leica Cryostate (CM 1850), some slides were subjected to Hematoxylin-Eosin (H&E) staining for assessing gross tissue reactions to nanoparticle implants, including cell accumulation, penetration and fibrotic capsule formation. All such experiments were repeated at least three times to ensure the reproducibility of our results.

Results and Discussion

A. Light scattering characterization of IPN nanoparticles

The hydrodynamic radius distribution ($f(R_h)$) of PINPAM and IPN nanoparticles at 23 °C are shown in Figure 1.[10] Here the polymer concentration of both PNIPAM and IPN water dispersions was about $5.0x10^{-5}$ g/ml and the pH was adjusted to ca. 6.5-7.5 for dynamic light scattering characterization. The PNIPAM and IPN nanoparticles were narrowly distributed with hydrodynamic radii (R_h) around 125 nm and around 155 nm, respectively. The IPN formation may be understood in terms of polymerization of acrylic acid within each PNIPAM microgel. The interaction between the –COOH group on acrylic acid and the –CONH- group on PNIPAM, in the form of monomeric or dimeric hydrogen bonding,[14] caused the preferred growth of the PAAc network around the PNIPAM network. The IPN particles had a larger size than their precursor PNIPAM particles because PAAc absorbs more water.

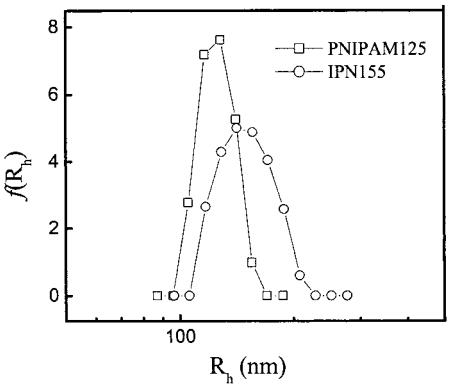

Figure 1. Hydrodynamic radius distributions of IPN nanoparticles (IPN155) and their precursors PNIPAM nanoparticles (PNIPAM125) in water at 23 °C, measured by the dynamic light scattering method.[10] Polymer concentrations and pH for both dispersions were adjusted, respectively, to 5.0 x 10^{-5} g/ml and ca. 6.5-7.5. Reproduced with permission from Ref. 10.

The values of R_h of IPN and PNIPAM nanoparticles in diluted dispersions with polymer concentration of 1.0 x 10^{-5} g/ml were measured by dynamic light scattering as a function of temperature.[10] They underwent the volume phase transition at the same temperature of about 34°C. For a randomly co-polymerized PAAc/PNIPAM gel, however, the volume phase transition temperature increases with PAAc concentration. [15] The relative size change of the IPN below and above the volume transition temperature was 24%, smaller than the 64% of the PNIPAM particles. Because the PAAc network in the IPN particle is not sensitive to the temperature and remained hydrophilic in this temperature range (21 to 40°C) at pH 7; this prevents collapse of the PNIPAM network.

B. Aqueous dispersions of IPN nanoparticles

The aqueous dispersions of the IPN nanoparticles exhibit rich phase behavior as shown in Figure 2. In the intermediate polymer concentration range (between 2.2 and 3.0x10^{-2} g/ml), the IPN dispersions are colloidal crystal fluids at 23 °C (Fig. 2A). These crystals are easy to observe due to their iridescent patterns caused by Bragg diffraction. [8] As the temperature increased, the dispersion became a fluid at 32 °C (Fig. 2B). At 37 °C, the dispersion couldn't flow even if the tube was set upside down (Fig. 2C).

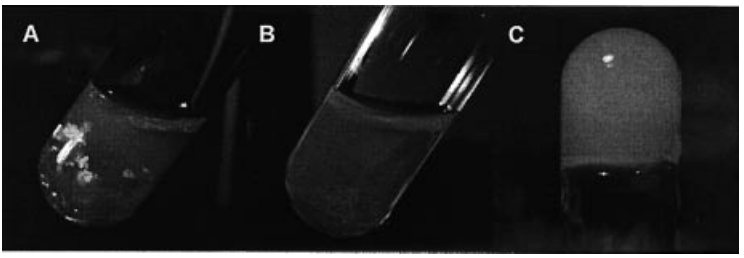

Figure 2. The viscosity change of the aqueous solution of IPN nanoparticles with polymer concentration of $2.5x10^{-2}$ g/ml. The dispersion is a crystal at 23 °C, a fluid at 32 °C (B) but becomes a gel at 37 °C (C). The color of the dispersion is due to the Bragg diffraction from an ordered array of colloidal particles in water.

The viscosity of an IPN nanoparticle dispersion with polymer concentration at 3.27 wt % was measured using a Brookfield viscometer as shown in Figure 3.[8] The viscosity of a PNIPAM nanoparticle dispersion with the same polymer concentration was also shown in the same figure as comparison. The viscosity of the PNIPAM nanoparticle dispersion (C=3.27 wt %) decreased as the temperature increased and reached a minimum plateau above 32°C. In contrast, the viscosity of the PNIPAM-PAAc IPN dispersion drastically increased, resulting in gelation above 33°C. It was found that the inverse thermoreversible gelation occurred in a broad polymer concentration above $2.5x10^{-2}$ g/ml.[8] That is, when the system is heated to above the gelation temperature T_g, it undergoes a transformation from a low-viscosity fluid to a gel. This behavior is completely reversible. In contrast to the graft copolymer of PAAc-g-PNIPAM and other thermothickening systems,[16] the semi-dilute IPN nanoparticle aqueous dispersions exhibited a sharper viscosity increase across the transition temperature.

The gelation of the IPN dispersion at $T>T_g$ may be caused by the attractive interactions between particles. Both van der Waals interaction and hydrophobic interaction may contribute to the attractive forces. At room temperature, PNIPAM particles are in the swollen state and they contain 97% water by volume. The van der Waals attraction between colloidal particles is negligible due to the close match in the Hamaker constants of the particles and the water. [17] The reduced osmotic second virial coefficient exhibits a sharp change at the volume transition temperature, beyond which it turns negative. Thermodynamic calculation indicates that the reduced interaction potential

energy between nanoparticles increases by over six orders of magnitude as temperature changes from 24°C to 36 °C, with the sharpest increase near the volume transition temperature of 34 °C.[17] The gelation may be achieved by the balance between van der Waal interaction and hydrophobic interaction between PNIPAM networks and the ionic repulsion of the PAAc networks in the IPN particles.

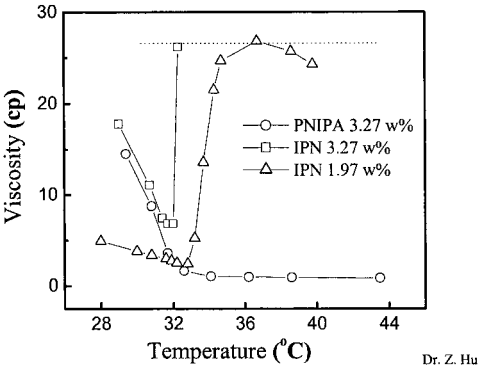

Figure 3. Temperature-dependent viscosity.[8] Viscosities of aqueous solutions of IPN (C=1.97 w%), IPN (C= 3.27 w%) and PNIPAM (C=3.27 wt%) were measured as a function of temperature using a Brookfield Viscometer. Reproduced with permission from Ref. 8.

C. Controlled drug release

One of the key applications of this novel hydrogel nanoparticle dispersion is in the area of controlled drug delivery. Dextran markers of various molecular weights were used as model macromolecular pseudodrugs and mixed with an IPN nanoparticle dispersion. At room temperature, the dispersion was a viscous fluid and was mixed with a dextran solution thoroughly. The drug-solution mixture was then heated to 37°C, at which point the dispersion becomes a gel. This gel was then taken out of the tube and immersed into a phosphate buffered saline (PBS) solution at 37°C.

The cumulative dextran release from the IPN155 gel with particle radius of 155 nm and polymer concentration of 5.25 wt% was measured using a UV-Visible spectrophotometer as a function of time as shown in Figure 4.[10] It was clear that the molecules with smaller molecular weights diffused out faster than those of higher molecular weights. The release rates slowed down gradually for 500K and 2M pseudodrug analogs according to their

molecular weights. In contrast to hydrogels obtained from polymer solutions with inverse thermoreversible gelation,[7] the hydrogel formed with our nanoparticle dispersions has a unique two-level structural hierarchy: the primary network consists of crosslinked polymer chains inside each nanoparticle, while the secondary network is a crosslinked system of the nanoparticles. The drug could be entrapped either between the particles or inside each particle.

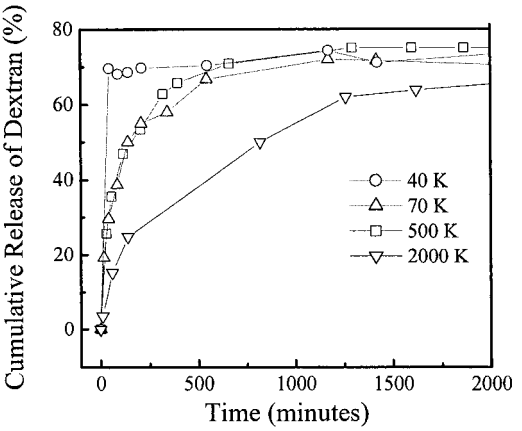

Figure 4. The dextran release profile from 5.25w% IPN155 nanoparticle network in 50 mM phosphate buffered saline (PBS) at pH 7.4 at 37°C.[10] The dextran markers with different molecular weights of 40K, 70K, 500K and 2000K were used as model macromolecule pseudodrugs. The weight ratio of PNIPAM to PAAc in each IPN nanoparticles was 1:0.50, as determined by the evaporation method. Reproduced with permission from Ref. 10.

D. Biocompatibility Test

To determine tissue responses to different materials, a mouse subcutaneous implantation model was used.[18] In fact, the subcutaneous cavity has been used as one of the main implantation models for controlled drug delivery.[19-21] After implantation for seven days, the implants and surrounding tissues were recovered for histological analyses and quantification. We find that nanoparticle assembly prompts minimal or no inflammatory responses and fibrotic tissue formation (Figures 5A, 5B, 5C & 5D). There is a very weak inflammatory response on the outer side of the implants (Figure 5B). Furthermore, no inflammatory cell found in the nanoparticle network indicates that

nanoparticle gel has a smaller pore size than required for cell migration (Figure 5C). Finally, on the muscle-side of the implants, we only find one layer of host cells indicating that this novel nanoparticle network has excellent tissue compatibility (Figure 5D).

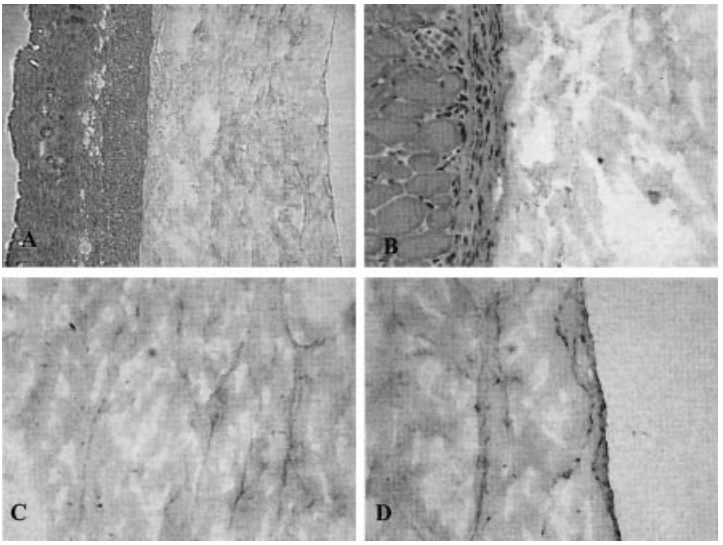

Figure 5. Histopathological analysis of the tissue compatibility of IPN155 nanoparticle network (H&E). Skin section from implant-bearing mice (magnification: 10X) shows that this nanoparticle network prompts minimal foreign body reactions (A). Close up pictures (40X) show that there is a very weak inflammatory cell accumulation on the outer side of the implant (B), almost no cell penetration in the nanoparticle network implants (C), and only one layer of inflammatory cells on the muscle-side of the nanoparticle network implants (D).

Overall, we find that hydrogel nanoparticle network implants possess excellent tissue compatibility. Rather surprisingly, the tissue compatibility of this nanoparticle network is even superior to hydrogel nanoparticles alone, at least PNIPAM (unpublished results). The real cause for differential tissue responses to nanoparticles and to nanoparticle network is not clear. We believe that the physical space between nanoparticles might provide space for fibrin deposition which then triggers the recruitment and accumulation of inflammatory cells.[22-23] On the other hand, possibly due to the quick solidification properties, nanoparticle gel may have less dead space which allows the accumulation of fibrin clot

and inflammatory cells, and subsequent fibrotic tissue formation. The results from this study suggest that PNIPAM nanoparticle network elicits the least inflammatory cell accumulation and fibrotic tissue formation. This observation suggests that the IPN155 nanoparticle network may serve as a good carrier for the applications of controlled delivery.

Conclusion

A novel aqueous dispersion of hydrogel nanoparticles with interpenetrating polymer networks of PNIPAM and PAAc has been synthesis and it can form a hydrophobically bonded nanoparticle network above its gelation temperature. This system exhibits a very rich phase behavior including an inverse thermoreversible gelation for polymer concentrations above $2.5x10^{-2}$ g/mL. Pseudodrug solutions have been easily mixed with a hydrogel nanoparticle dispersion at room temperature and are released slowly from the gel depot at body temperature. As a result, the pseudodrug is entrapped between the particles. Dextran markers of various molecular weights were used as model macromolecular pseudodrugs to obtain the releasing profiles for a series of semi-diluted IPN dispersions at 37°C, as measured by UV/Visible spectrometer. Such a nanoparticle dispersion can be easily injected into animals via a 30 gauge or larger needle. Shortly after implantation, this dispersion undergoes *in situ* solidification triggered by body temperature (37 °C). This nanoparticle network has excellent bio- and tissue-compatibility at least in the mice subcutaneous implantation model.

Acknowledgements

ZH thanks the financial support from the National Science Foundation under Grant No. DMR-0102468, the U.S. Army Research Office under Grant No. DAAD 19-01-1-0596. LT gratefully acknowledges the financial support from the American Heart Association and the National Institutes of Health.

[1] J. M. Guenet, Thermoreversible Gelation of Polymers and Biopolymers, Academic Press, London, **1992**.
[2] G. Franz, Polysaccharides in pharmacy, Adv. Polym. Sci. **1986**, 76, 1.
[3] P.G. Higgs, R.C. Ball (Eds.), Physical Network, Polymers and Gels, Elsevier, New York, **1990**, pp. 185.
[4] B. Jeong, S. W. Kim, Y. H. Bae, Adv. Drug Del. Rev. **2002**, 54, 37.
[5] A. Chenite, C. Chaput, D. Wang, C. Combes, M.D. Buschmann, C.D. Hoemann, J.C. Leroux, B.L. Atkinson, F. A. Selmani, Biomaterials **2000**, 21, 2155.
[6] P. Alexandridis, T. A. Hatton, Colloids Surfaces A: Physicochem. Eng. Aspects **1995**, 96, 1.
[7] C. K. Han, Y. H. Bae, Polymer **1998,** 39, 2809.
[8] Z. B. Hu and X. H. Xia, Advanced Materials **2004**, 16**,** 305.
[9] X. H. Xia and Z. B. Hu, Langmuir **2004**, 20, 2094.
[10] X. H. Xia, Z. B. Hu and M. Marquez, J. Controlled Release **2004,** (in press)
[11] Z. B. Hu, X. H. Lu, J. Gao, and C. J. Wang, Advanced Materials **2000**, 12, 1173
[12] Z. B. Hu, X. H. Lu and J. Gao, Advanced Materials **2001,** 13, 1708
[13] R. H. Pelton, P. Chibante, Colloids Surf. **1986,** 20, 247.
[14] F. Ilmain, T. Tanaka, E. Kokufuta, Nature **1991**, 349, 400
[15] S. Hirotsu, Y. Hirokawa, T. Tanaka, J. Chem. Phys. **1987**, 87, 1392.
[16] A. Durand, D. Hourdet, Polymer **1999**, 40, 4941.
[17] J. Z. Wu, B. Zhou, and Z. B. Hu, Phys. Rev. Lett. **2003**, 90, 048304; J. Wu, G. Huang, Z. B. Hu, Macromolecules **2003,** 36, 440.
[18] H. Weng, J. Zhou, L. Tang, Z. B. Hu, J. Biomaterials Sci. Polym. Ed. **2004**, 15, 1167.
[19] V. Srinivasan, J. A. Pendergrass, K. S. Kumar, M. R. Landauer, T. M. Seed, Int. J. Radiat. Biol. **2002**, 78, 535.
[20] Z. Cui, R. J. Mumper, Int. J. Pharm. **2002**, 238, 229.
[21] A. Prokop, E. Kozlov, G. W. Newman, M. J. Newman, Biotechnol. Bioeng. **2002**, 78, 459.
[22] L. Tang, J. W. Eaton, Molecular Medicine **1999**, 5, 351.
[23] W. J. Hu, J. W. Eaton, L. Tang, Blood **2001**, 98, 1231.